Eur. Phys. J. C (2024) 84:210
https://doi.org/10.1140/epjc/s10052-024-12572-5

THE EUROPEAN PHYSICAL JOURNAL C

Regular Article - Theoretical Physics

Repeating fast radio bursts produced by a strange star interacting with its planet in an eccentric orbit

Nurimangul Nurmamat[1,a], **Yong-Feng Huang**[1,2,3,b], **Jin-Jun Geng**[4,c], **Abdusattar Kurban**[3,5,d], **Bing Li**[6,7,e]

[1] School of Astronomy and Space Science, Nanjing University, Nanjing 210023, China
[2] Key Laboratory of Modern Astronomy and Astrophysics (Nanjing University), Ministry of Education, Nanjing 210023, China
[3] Xinjiang Astronomical Observatory, Chinese Academy of Sciences, Urumqi 830011, Xinjiang, China
[4] Purple Mountain Observatory, Chinese Academy of Sciences, Nanjing 210023, China
[5] Xinjiang Key Laboratory of Radio Astrophysics, Urumqi 830011, China
[6] Key Laboratory of Particle Astrophysics, Chinese Academy of Sciences, Beijing 100049, China
[7] Particle Astrophysics Division, Institute of High Energy Physics, Chinese Academy of Sciences, Beijing 100049, China

Received: 15 September 2023 / Accepted: 18 February 2024 / Published online: 29 February 2024

Abstract FRB 180916 is an important repeating fast radio burst (FRB) source. Interestingly, the activity of FRB 180916 shows a well-regulated behavior, with a period of 16.35 days. The bursts are found to occur in a duty cycle of about 5 days in each period. In this study, we suggest that the bursts of FRB 180916 are produced by a strange star interacting with its planet. The planet moves in a highly eccentric orbit around its compact host, with the periastron only slightly beyond the tidal disruption radius. As a result, the planet will be partially disrupted every time it passes through the periastron. The stripped material from the planet will be accreted by the strange star, falling to the polar cap region along the magnetic field lines and accumulated there. It will finally lead to a local collapse when the crust at the polar region is overloaded, triggering an FRB. The observed 16.35 day period corresponds to the orbital motion of the planet, and the 5 day duty cycle is explained as the duration of the partial disruption near the periastron. The energy released in each local collapse event can be as high as $\sim 10^{42}$ erg, which is large enough to account for typical FRBs even if the radiation efficiency is low.

1 Introduction

Strange quark matter (SQM), which contains almost equal number of up, down and strange quarks, may be the true ground state of hadrons [1]. If this SQM hypothesis is true, then there should exist strange quark stars (also commonly shortened as strange stars (SSs)). SSs are extremely compact stellar objects that are mainly composed of SQM [2–4]. Comparing with traditional neutron stars (NSs), an SS may have an even higher mean density. SSs may be connected with various high energy astronomical phenomena, such as millisecond magnetars, X-ray or γ-ray bursters, Quark-nova, etc. [5–10]. However, it is very difficult to distinguish between SSs and NSs via observations. The main reason is that SSs may be covered by a thin crust of normal hadronic matter [2], which makes SSs to be very much similar to NSs for an outside observer. The total mass of an SS crust is believed to be in the range of 10^{-7}–$10^{-5}\,M_{\odot}$, with a thickness of $\sim 2\times10^{4}$ cm. Huang et al. [11,12] numerically calculated the mechanical equilibrium condition at the bottom of the crust, and found that the maximum density at the crust bottom should be much smaller than the so called neutron drip density. As a result, a typical $1.4\,M_{\odot}$ SS cannot have a crust more massive than $M_{\rm crust}\sim 3.4\times10^{-6}M_{\odot}$, with the crust thickness being less than $\sim 10^{4}$ cm. In this case, when an SS accretes matter from the surrounding medium, the crust will get heavier and heavier, which may finally lead to the collapse of the crust in a very short time ($\sim 5.4\times10^{-3}$ s), producing an intense explosion of short duration. During the collapse, normal hadronic matter is converted to SQM, and each baryon will release an energy of ~ 6.3 MeV. The total energy will roughly be 10^{46}–10^{47} erg [13].

Fast radio bursts (FRBs) are a new kind of high energy astronomical phenomena characterized by a short duration ($\sim$ a few milliseconds) and intense emission in radio waves [14]. Their extra-galactic origin was firstly hinted from the

[a] e-mail: nurimangul@smail.nju.edu.cn
[b] e-mail: hyf@nju.edu.cn (corresponding author)
[c] e-mail: jjgeng@pmo.ac.cn
[d] e-mail: akurban@xao.ac.cn
[e] e-mail: libing@ihep.ac.cn

large dispersion measure (DM) along the line of sight, and is later confirmed by direct redshift measurement in a few cases [15–17]. It is interesting to note that some FRB sources can burst out repeatedly, even with periodicity being hinted in several of them. Till now, nearly 800 different FRB sources have been detected, among which more than 60 are repeaters [18–21]. [1] The host galaxies are also identified for 44 sources [22][2]. However, the central engine and trigger mechanism of FRBs are still largely uncertain. It is widely believed that FRBs should be connected with magnetars, and may be connected with some kinds of perturbations in the magnetosphere [23,24]. In addition to that, various other models have also been proposed and could not be expelled yet [25]. For example, motivated by the atmosphere pollution of white dwarfs (WDs) by heavy elements [26] and the WD-planet/asteroid tidal disruption interactions [27,28] proposed that periodically repeating FRBs may be triggered by a magnetized NS interacting with its planet in a highly eccentric orbit. The planet will be partially tidal disrupted every time it comes to the periastron. The disrupted clumps then interact with the pulsar wind and produce FRBs via the Alfvén wing mechanism.

More interestingly, Zhang et al. [29] argued that FRBs may be triggered by the collapse of SS crust when the SS accretes matter from the surrounding environment. In their study, the crust collapses as a whole to release a huge amount of energy, but which also makes it difficult to produce FRBs repeatedly. Recently, Geng et al. [30] went further to argue that the accreted matter will not diffuse on the crust due to the strong surface magnetic field. As a result, only the crust at the polar cap region will collapse when it is locally overloaded. In this way, an SS accreting from its companion can naturally produce periodic FRBs, such as the repeating source of FRB 180916. Note that in their framework, the periodicity is mainly due to the thermal-viscous instability of the accretion disk. As a result, the active window ($\sim$ 5 days for FRB 180916) corresponds to a high accretion state of the system, while the $\sim$ 16 day period corresponds to the accumulation timescale of the accretion disk. Both the active window and the period are determined by the accretion rate and the viscosity parameter. Note that since the periodicity comes from the thermal-viscous instability, the period may not be stable and may vary in a relatively wide range.

In this study, the essential ingredients of Kurban et al.'s [28] and Geng et al.'s [30] models are incorporated to build a new model for periodically repeating FRBs. We assume that a planet moves around a magnetized SS in a highly eccentric orbit. The planet will be partially disrupted by tidal force every time it comes across the periastron. The disrupted material is then accreted by the SS, causing the polar cap to collapse and produce FRBs. Note that the planet can be either a gaseous or a rocky one. For a gaseous planet, it is easy to understand that the accreted material will fall toward the polar regions of the SS along the magnetic field lines. For a rocky planet, the partial disruption process occurs at a distance of $\sim 10^{11}$ cm, producing rocky clumps a few kilometers in size. Shearing strength then plays the major role to resist the tidal force for these clumps. However, they will also be completely disrupted by the tidal force when their distance to the SS is $\sim 10^{9}$ cm. Thus they will still fall toward the polar regions along the magnetic field lines [31].

The structure of our paper is organized as follows. In Sect. 2, the basic features of highly eccentric planetary systems are introduced. The collapsing process of the polar cap crust of an accreting SS is presented in Sect. 3. In Sect. 4, the model is applied to explain the observed repeating event of FRB 180916. Finally, Sect. 5 presents our conclusions and some discussion.

2 Tidal disruption in a highly eccentric planetary system

When an object gets too close to a compact star, it will be teared apart and a tidal disruption event happens. In such a process, a significant portion of the teared matter will be captured and accreted by the compact star [32–34]. In a tidal disruption event, the compact star can be a BH, NS or WD, and the teared object can be a main sequence star, a planet, an asteroid/comet, or sometimes even a WD [26,27,35–37]. Recently, Kurban et al. [28] studied the interaction of a highly magnetized NS with and its planet in a highly eccentric orbit. They suggested that the planet will be partially disrupted when it passes through the periastron. The disrupted clumps then interact with the magnetar wind to give birth to FRBs.

In this study, we adopt the basic configuration of [28]. The main difference is that we use a strange star to replace the compact star of NS. The planet is still in a highly eccentrical orbit. It will be partially disrupted by the SS every time it passes through the periastron. The teared materials are then accreted by the SS, falling toward the magnetic polar regions. The accumulated materials will finally lead to a local collapse of the SS crust at the polar region, producing an FRB.

We assume that the SS has a typical mass of $M_{\rm ss} = 1.4 M_{\odot}$. The companion is a planet with the mass denoted as $m_{\rm planet}$ and the mean density denoted as $\bar{\rho}$. The semimajor axis and period of its orbit are denoted as a and $P_{\rm orb}$, respectively. According to the Kepler's third law, the orbital period

[1] http://blinkverse.alkaidos.cn/#/overview.

[2] https://ecommons.cornell.edu/server/api/core/bitstreams/3c93d0f8-c307-4909-a9a0-26b7a2df1397/content.

of this planetary system can be expressed as

$$P_{\rm orb} = \left(\frac{4\pi^2 a^3}{G\left(M_{\rm ss} + m_{\rm planet}\right)}\right)^{\frac{1}{2}}, \quad (1)$$

where G is the gravitational constant. The separation (R) between the SS and the planet in the eccentric orbit is related to the eccentricity (e), semimajor axis (a) and phase (θ) as $R = a(1-e^2)/(1+e\cos\theta)$, while the periastron separation of the planet is $R_{\rm p} = a(1-e)$.

The tidal disruption radius ($R_{\rm T}$), i.e., the separation at which the planet will be completely disrupted by the tidal force of the compact star [32], is $R_{\rm T} = (6M_{\rm SS}/\pi\bar{\rho})^{1/3}$. When the separation is slightly larger, i.e. $R_{\rm T} < R < 2.7\,R_{\rm T}$, the planet will be partially disrupted [38]. In the highly eccentric orbit case considered here, the planet will be significantly affected by the tidal force near the periastron, but will be unaffected at other orbital phase. Note that if the periastron is too close to the SS (i.e., with $R_{\rm p} \le R_{\rm T}$), the planet will be completely disrupted when it passes through the periastron. On the other hand, if $R_{\rm T} < R_{\rm p} < 2.7\,R_{\rm T}$, the planet will only be partially disrupted every time it passes through the periastron. In this study, we take $R_{\rm p} = 1.5\,R_{\rm T}$ as a typical case for the partial disruption configuration. Also, we only consider the tidal interaction near the periastron for simplicity. The condition of $R_{\rm p} = 1.5\,R_{\rm T}$ then means

$$a\,(1-e) = 1.5\left(\frac{6M_{\rm ss}}{\pi\bar{\rho}}\right)^{\frac{1}{3}}. \quad (2)$$

Because our condition of $R_{\rm p} = 1.5\,R_{\rm T}$ satisfies the partial disruption condition ($R_{\rm T} < R_{\rm p} < 2.7\,R_{\rm T}$), there exists a critical phase angle $\theta_{\rm c}$ defined by $R(\theta_{\rm c}) = 2.7\,R_{\rm T}$. When the planet is in the phase range of $-\theta_{\rm c} < \theta < \theta_{\rm c}$, it will be seriously affected by tidal interaction and the system will be in an active regime. Therefore, the active period can be expressed as [28,39]

$$\Delta P_{\rm orb} = \frac{P_{\rm orb}}{2\pi}\sqrt{(1-e^2)^3}\int_{-\theta_{\rm c}}^{\theta_{\rm c}} \frac{1}{(1+e\cos\,\theta)^2}\,d\theta. \quad (3)$$

The partial disruption is a very complicated process. It is difficult to estimate how much material will be teared up from the planet and will be finally accreted by the SS. It may depend on a lot of complicated factors, such as the composition of the planet and its rotation. Here, we roughly estimate the total accreted mass during one active period as $M_{\rm acc} = \Delta P_{\rm orb}\dot{M}_{\rm Edd}$, where $\dot{M}_{\rm Edd}$ is the Eddington accretion rate expressed as $\dot{M}_{\rm Edd} = 4\pi r m_{\rm p} c/\sigma_{\rm T} \cong 10^{18}\,{\rm g\,s^{-1}}$. Here r is the radius of the SS, $m_{\rm p}$ is the mass of proton, c is the speed of light, and $\sigma_{\rm T}$ is the cross section of Thomson scattering.

3 Collapse of the SS crust at polar region

SSs are compact objects made up of almost equal numbers of up, down and strange quarks. They may be covered by a normal matter crust [2]. The maximum density at the bottom of the crust should not exceed the definite limit of neutron drip density ($\epsilon_{\rm drip}$), but is most likely significantly less than that when the mechanical equilibrium is considered [11,12]. As a result, the maximum mass of the crust of a typical 1.4 $M_\odot$ SS is $M_{\rm crust} \sim 3.4\times10^{-6}\,M_\odot$, with a thickness of $\sim 10^4$ cm.

When an SS accretes material from the surrounding medium, the crust will be heavier and heavier and may finally collapse in a very short time ($\sim 10^{-3}$ s). During the collapse, every baryon may release an energy of about 6.3 MeV when it is converted into SQM, and the total energy released due to the collapse of the whole crust can be as high as 10^{46}–10^{47} erg [13], leading to an intense short explosion. Zhang et al. [29] argued that an FRB could be produced during the crust collapse. However, if the SS has a strong dipolar magnetic field, then the accreted material will fall toward the polar region along the magnetic field lines and accumulates there. In this case, only the polar region is overloaded and it may lead to a local collapse rather than the collapse of the whole crust. Cheng et al. [7] suggested that such a local collapse can interpret the quasi-periodic hard X-ray bursts from GRO J1744-28. Very recently, Geng et al. [30] also used the fractional collapse of an SS crust to explain periodical repeating FRBs. In their model, the SS accretes matter from a close-in companion star. The accreted matter also accumulates at the two polar regions, leading to a local collapse when the crust at the polar region is too heavy. Note that the periodical behavior of FRBs is caused by the thermal instability of the accretion disk, thus the repeating period is not very strict. It is worth mentioning that the polar cap is a surface region of the compact star determined by the open magnetic field lines [40–43].

In this study, we consider the interaction between an SS and its planet near the periastron. The planet is partially disrupted there and the stripped material is accreted by the SS, falling to the two polar cap regions and accumulated on the crust. It may finally lead to a local collapse of the polar cap region, producing an FRB. A schematic illustration of our model is presented in Fig. 1.

In our study, we take the SS mass, radius and total crust mass as mentioned above, with a crust thickness of $\ell \sim 2\times10^4$ cm. Then the mass of the crust at the polar cap region is approximately

$$M_{\rm pl,crust} = \frac{\pi\theta_{\rm cap}{}^2}{4\pi}M_{\rm crust}, \quad (4)$$

where $\theta_{\rm cap}$ is the half opening angel of the polar cap. It can be estimated by $\theta_{\rm cap} \approx (2\pi r/cP)^{1/2} \sim 1.45\times10^{-2}P_0^{-1/2}r_6^{1/2}$, where P is the rotation period of the SS. $\theta_{\rm cap}$ implies a filling

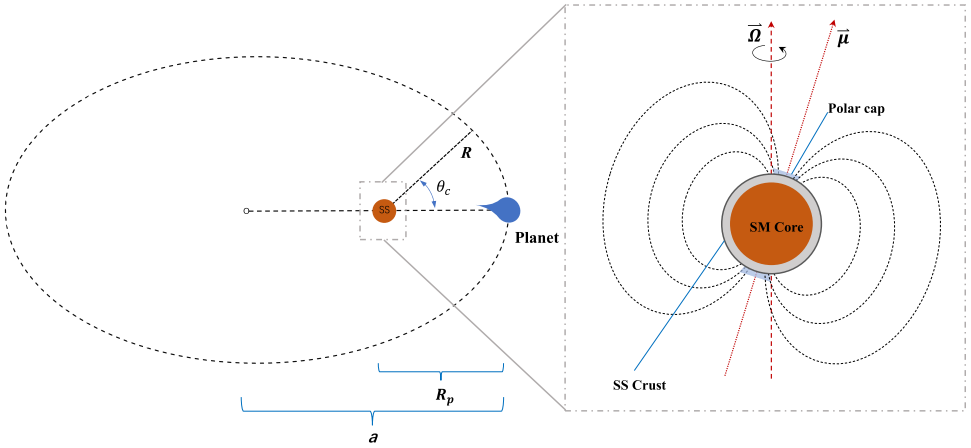

Fig. 1 A not-to-scale schematic illustration of our model. The left portion shows that a planet is moving around an SS in a highly eccentric orbit. It will be partially disrupted when passing through the periastron. The right portion is an enlargement of the SS. It shows that the accreted material accumulates at the polar cap region of the SS, finally leading to a local collapse of the crust. Here $\boldsymbol{\mu}$ and $\boldsymbol{\Omega}$ indicate the magnetic axis and rotation axis of the SS, respectively

factor of the surface of $f \approx \theta_{\rm cap}^2/4$ [44,45]. Assuming each hadron can release an energy of ~ 6.3 MeV when it is converted to quark matter, the total energy released during the local collapse of the polar cap region is

$$E_{\rm c,tot} = \frac{M_{\rm pl,crust}}{m_{\rm p}} \times 6.3\,{\rm MeV}, \tag{5}$$

where $m_{\rm p}$ is the mass of proton.

The energy is released on a short timescale [13], leading to the formation of a fireball of electron/positron ($e^{\pm}$) pairs. The electrons/positrons streams outward along the open magnetic field lines, producing a thin shell in the magnetosphere. They will finally give birth to an FRB through coherent emission [29]. Note that only a small portion of the energy of $E_{\rm c,tot}$ will go into the FRB due to the limited energy conversion efficiency in the process. Denoting the energy conversion efficiency as η, then the intrinsic energy of the FRB is $E_{\rm FRB} \sim \eta E_{\rm c,tot}$.

After the collapse of the polar cap crust, the stripped material from the planet will continue to fall toward the polar cap region. The broken crust can then be re-built to get ready for the next burst. Repeating FRBs can be produced in this way as long as the accretion continues. Note that in each collapse event, it is not necessary that all the matter of the polar cap crust must fall onto the strange core. It is quite possible that only a portion of the matter will do so that significantly less material is needed to restore the crust. We will further discuss this issue in the next section.

4 Comparison with FRB 180916

FRB 180916 is a periodically repeating FRB source. Till the end of 2021, a total of 44 bursts have been detected from this source [46]. During the active state, an event rate of about $0.9^{+0.5}_{-0.4}$ bursts per hour is reported. A period of 16.35 ± 0.18 days is found in its activities, with a ~ 5 day active window in each period [47]. Some plausible models have been proposed to explain this periodic behavior of FRB 180916 [48,49].

In this section, we use our model to explain the periodicity of FRB 180916. First, we take typical values for some model parameters, such as the SS mass and radius, and the total crust mass. For a typical spin period of $P = 1$ s, the crust mass at the polar cap region will be $M_{\rm pl,crust} \approx 3.55 \times 10^{23}$ g. The mass of the planet is taken as $m_{\rm planet} = 10^{-3}\,M_\odot$ and its mean density is taken as $\bar{\rho} = 10\,{\rm g\,cm^{-3}}$. The radius of the planet is then $R_{\rm planet} = \left(\frac{3m_{\rm planet}}{4\pi\bar{\rho}}\right)^{1/3}$.

In our framework, the observed period of 16.35 days in FRB 180916 is due to the orbital motion of the planet around the SS, i.e. $P_{\rm orb} = 16.35$ days. Then, from Eq. (1) in Sect. 2, we can derive the semimajor axis of the planet orbit as $a = \left[G(M_{\rm ss} + m_{\rm planet})P_{\rm orb}^2/4\pi^2\right]^{1/3} \simeq 2.11 \times 10^{12}$ cm. At the same time, the tidal disruption radius is $R_{\rm T} = (6M_{\rm ss}/\pi\bar{\rho})^{1/3} \simeq 8.08 \times 10^{10}$ cm. So, from Eq. (2), the orbital eccentricity is $e = 1 - 1.5\,R_{\rm T}/a \simeq 0.94$ correspondingly. Note that we have taken the pericenter distance as $R_{\rm P} = 1.5\,R_{\rm T} \simeq 1.21 \times 10^{11}$ cm. For the clumps that are generated from the planet's inner side, the periastron distance can be written as $R_{\rm P}^{\rm cl} = a_{\rm cl}\,(1 - e_{\rm cl})$, where $a_{\rm cl} = a\left(1 + a\frac{2R_{\rm planet}}{R_{\rm P}(R_{\rm P}+R_{\rm planet})}\right)$ and $e_{\rm cl} = 1 - \frac{R_{\rm P}-R_{\rm planet}}{a_{\rm cl}}$ are the semimajor axis and eccentricity of the clump, respectively [31]. Then the clumps' periastron distance is $R_{\rm P}^{\rm cl} \simeq 5.67 \times 10^{10}$ cm.

We assume that the SS has a very strong magnetic field of $B = 1 \times 10^{16}$ G and take the mass accretion rate as $\dot{m} = \dot{M}_{\rm Edd}$, then the magnetosphere radius of the SS can be calculated as $R_{\rm m} = \left(\frac{\mu^4}{2GM_{\rm ss}\dot{m}^2}\right)^{1/7} \simeq 3.09 \times 10^{10}$ cm, where $\mu = BR_{\rm ss}^3$ is the dipolar moment of the magnetic field. We see that the magnetosphere radius and the clumps' periastron distance is comparable, which indicates that the clumps would be seriously affected by the magnetic field. They will be quickly decelerated by the magnetosphere and be captured by the SS. In fact, if we consider a more compact planet with a higher density of $\bar{\rho} = 40\,{\rm g\,cm^{-3}}$ [50,51], then the clumps' periastron distance is $R_{\rm P}^{\rm cl} = 2.75 \times 10^{10}$ cm. It is even smaller than the magnetosphere radius, so that the clumps will be

effectively captured by the magnetic field and fall toward the polar cap region of the SS along the field lines. The falling timescale of the clumps (with a radius of $R_{\rm cl}$) from the magnetosphere radius to the vicinity of the SS can be roughly estimated as [52] $t_{\rm fb} = \frac{2\pi R_{\rm m}^3}{(GM_{\rm ss})^{1/2}(2R_{cl})^{3/2}}$. For a clump of the size of 2 km, the falling timescale is $t_{\rm fb} \backsimeq 0.51$ day. Therefore, with the help of the magnetic field, the clumps could be essentially captured by the SS and fall toward the polar region very soon.

For FRB 180916, the observed duty cycle of bursts is about 5 days. It corresponds to the duration of the partial disruption stage, i.e. the time consumed by the planet when it passes through the periastron. So, we have $\Delta P_{\rm orb} = 5$ days. Then, under the Eddington accretion limit, the mass of the matter accreted by the SS can be roughly estimated as $M_{\rm acc} = \Delta P_{\rm orb} \cdot \dot{M}_{\rm Edd} \simeq 4.32 \times 10^{23}$ g. We see that this mass is higher than the crust mass at the polar cap region ($M_{\rm pl,crust}$), which means that the accreted material will be sufficient to trigger at least one local collapse event. Note that during one single local collapse process, not all the material at the polar cap will necessarily fall onto the strange core. It is quite possible that only a fraction of the matter will collapse. In this case, an accreted mass significantly less than $M_{\rm pl,crust}$ will be enough to restore the polar cap region. It means that more than one FRB could be produced during one active cycle, which may account for the relatively high burst rate of FRB 180916 in an active window. However, it is very difficult to estimate the exact ratio of polar cap material collapsed in the process, which needs further investigation in the future.

More interestingly, recent observations reveal that the active window of FRB180916 can essentially be as large as one half of the period [53]. Of course, the event rate at phases other than the normal 5-day duration is significantly lower. This feature could also be explained in our framework. In our model, the partial disruption happens in a 5-day duration. The disrupted materials are then accreted by the SS. In realistic case, there should exist a dispersion in the falling time of the materials. Also, the accretion rate at later stages would be smaller, which also prolongs the accretion process. Therefore, the total duty cycle will be correspondingly longer than 5 days and can extend to one half of the period.

It should be noted that the periodicity of FRB 180916 is rather stable ever since the discover of this repeating source [54]. However, in our model, the mass loss of the planet may lead to a change in its orbital period. We thus need to examine this effect. In an interacting binary system, the companion star will expand its radius to adjust to a new equilibrium state after each partial disruption. The disruption radius will change correspondingly, which leads the period to change. For a normal companion star, such an effect has been studied in detail by several groups [55,56]. Here we follow Hamers and Dosopoulou [57] to calculate the evolution of the orbital period of the planet. The detailed calculation procedure is described in the Appendix section. Our numerical results for the evolution of the orbital period is shown in Fig. 2. We have considered four different mean densities for the planet, $\rho = 1, 3, 8, 10\,{\rm g\,cm^{-3}}$. Generally, we see that the period is relatively stable at early stages in all the cases. Especially, the period change is very small in 200–400 years. Also, the total mass loss of the planet is very small comparing to its original mass during this time. Thus our model is consistent with the stable periodicity observed in FRB 180916.

Taking $M_{\rm pl,crust} \approx 3.55 \times 10^{23}$ g, the collapse of the polar cap region will release a total energy of $E_{\rm c,tot} \approx 2.15 \times 10^{42}$ erg in one orbital period. The energy of FRBs can then be $E_{\rm FRB} \sim 2.15 \times 10^{38}$ erg even for a very small conversion efficiency of $\eta = 10^{-4}$. It is large enough to account for most observed bursts from FRB 180916. Furthermore, if the FRB emission is highly beamed, then the energy will be emitted into a very narrow solid angle. It means that the observer would see a much stronger burst (with a large isotropic-equivalent energy). Since the emissions of FRBs are coherent and strong magnetic fields are involved, the radiation should naturally be beamed, which significantly amplifies the isotropic-equivalent energy.

Recent observations indicate that the active window of FRB 180916 seems to be frequency-dependent [48,58,59]. FRB emissions have been detected from 1.4 GHz down to 120 MHz. In such a wide frequency range, the active window is chromatic, i.e., bursts with higher frequencies generally arrive earlier in phase. Such a frequency-dependent behavior could be explained in our framework. As described earlier in this section, the observed duty cycle of bursts corresponds to the duration of the partial disruption stage, i.e. the time taken for the planet to pass by the periastron. In this period, the stripped material from the planet will gather around the SS, producing a plasma cloud surrounding the compact star. The density of the plasma will decrease with time due to the accretion of the SS, which will lead to a decrease of the characteristic oscillation frequency of the plasma. As a result, low frequency FRBs cannot penetrate through the plasma at early stages of the active period. They are detectable only when the plasma's characteristic oscillation frequency becomes small enough at relatively late stages of the duty cycle.

To present a more detailed explanation of the process, let us assume that the accretion of the clump debris by the SS follows the normal $t^{-5/3}$ rule of tidal disruption events [33,60]. Then, the accretion rate varies with time as $\dot{m} \sim \dot{M}_{\rm fb}\left(\frac{t}{t_{\rm fb}}\right)^{-5/3}$, where $\dot{M}_{\rm fb}$ is the accretion rate at the fallback time ($t_{\rm fb}$). Consequently, the plasma density around the SS also decays as $n_{\rm e} \sim n_{\rm e0}\left(\frac{t}{t_{\rm fb}}\right)^{-5/3}$, where $n_{\rm e0}$ is the density at $t_{\rm fb}$. The characteristic oscillation frequency of the plasma can then be calculated as $\omega_{\rm p} = \left(\frac{4\pi n_{\rm e} e^2}{m_{\rm e}}\right)^{1/2} \simeq$

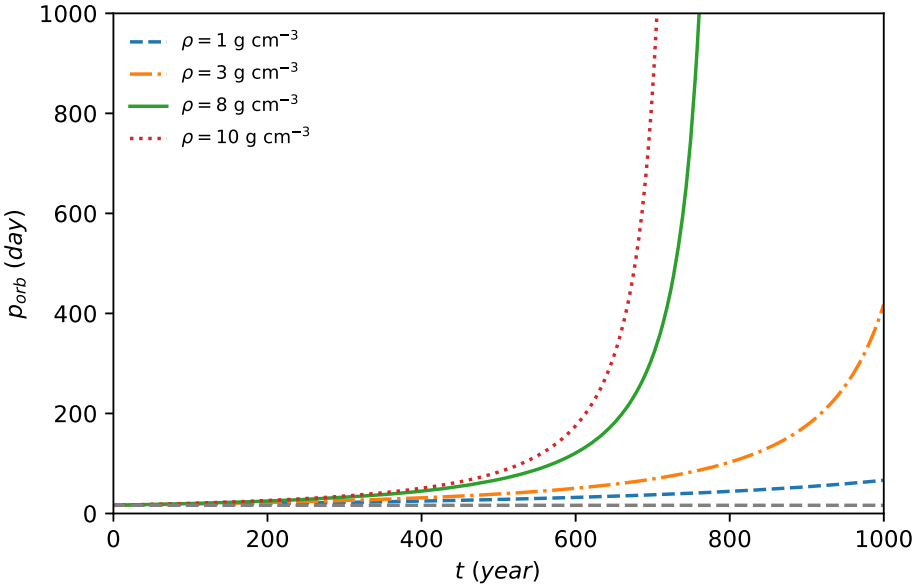

Fig. 2 Long-term evolution of the orbital period of the planet. We take the parameters as $m_{\rm planet} = 10^{-3}\,{\rm M}_\odot$, $M_{\rm ss} = 1.4\,{\rm M}_\odot$, and $R_{\rm p} = 1.5R_T$. The initial period is taken as $P_{\rm orb} = 16.35$ days, which is shown by the dashed horizontal line. Different mean densities are assumed for the planet, which are marked in the figure

$\left(5.63 \times 10^4\,{\rm s}^{-1}\right) n_{\rm e}^{1/2}$, where $n_{\rm e}$ is in units of cm^{-3} in the last expression. Assuming that most of the material falls onto the SS to produce the FRBs and only a fraction of 10% still remains in the magnetosphere initially, then the density of the remnant plasma can be estimated as $n_{\rm e0} = \frac{3m_{\rm cl}}{40\pi R_{\rm cl}^3 m_{\rm P}}$. For typical clumps with $R_{\rm cl} = 2$ km and $m_{\rm cl} = 1.34 \times 10^{18}$ g, the initial plasma density is $n_{\rm e0} = 6.49 \times 10^8$ cm^{-3} and the corresponding characteristic frequency is $\omega_{\rm p} = 1.43 \times 10^9$ Hz. Taking $t_{\rm fb} = 0.5$ days, the plasma density will decrease to $n_{\rm e} = 6.66 \times 10^7$ cm^{-3} two days later, and the corresponding characteristic oscillation frequency is 0.46×10^9 Hz. We see that the plasma frequency decreases significantly during the duty cycle. It means that high frequency FRBs could penetrate through the magnetosphere and would be detected at the early stage of the duty cycle. However, low frequency events will be absorbed by the plasma at early stages. They could be detected mainly at later stages, when the plasma density becomes smaller. Such a picture is well consistent with the frequency-dependent active window as observed in FRB 180916.

Note that there a small random variation of the dispersion measure (DM) observed in FRB 180916. Its amplitude is of the order of $\sim 1\,{\rm pc\,cm}^{-3}$. In our model, additional electrons will be emitted from the polar cap region when the crust collapses to produce an FRB, the mean density of which can be estimated as $n_{\rm e} = \frac{\zeta E_{\rm c,tot}}{\delta t} \frac{1}{4\pi m_{\rm p} c^3 R_{\rm FB}^2 2\Gamma^2}$, where δt is the burst duration, $R_{\rm FB}$ is the typical radius of the electron cloud, η is the radiation efficiency, and Γ is the Lorentz factor of electrons. Taking $\eta \sim 10^{-4}$, $\delta t \sim 10$ ms, $\Gamma = 100$, and $R_{\rm FB} \sim 1 \times 10^8$ cm, the mean electron density of the fireball will be $n_{\rm e} \sim 6.4 \times 10^{10}\,{\rm cm}^{-3}$. It will lead to an additional DM of $\sim 2\,{\rm pc\,cm}^{-3}$, which is roughly consistent with the variation amplitude of the observed DM.

Furthermore, for FRB 180916, the subpulses are found to show a downward drifting behavior on the time-frequency diagram. It could be easily explained by considering the radius-to-frequency mapping in our framework. In our scenario, the radio emission comes from the coherent curvature radiation of pairs along open magnetic field lines, then the later subpulses usually have a lower characteristic frequency since they are emitted at higher latitudes [61]. It is quite similar to the radio emission of pulsars.

Observations show that FRB 180916 has an obvious secular increase in the rotation measure ($\Delta RM \sim 50$ rad/m^{-2}) over the 9-month period from 2021 April to 2021 December [62]. Long-term rotation measure (RM) variabilities have been explained in the framework of massive binary systems [63,64]. However, the secular RM variability of FRB 180916 is not associated with any significant DM variability, nor does it be connected with the periodicity and active window variations [54,62]. Such a RM variation thus is not a natural outcome of binary interactions, including our model. We suggest that it could be caused by some environmental effects. It is possible that there are some inhomogeneous magnetic fields around the FRB source, which lead to the change of RM as the line of sight changes due to the proper motion of the SS.

5 Conclusions and discussion

In this study, a new model is proposed to explain the periodical behavior of FRB 180916. We consider the interaction between an SS and a planet. The planet is assumed to move around the SS in a highly eccentric orbit, with an eccentricity of $e = 0.94$. The orbital period is 16.35 days, which just corresponds to the observed period of FRB 180916. The periastron of the planet satisfies the condition

of $R_T < R_p < 2.7R_T$, so that it will be partially disrupted by tidal force of the SS every time it passes through the periastron. The duration of such a tidal interaction near the periastron is about 5 days in each period, which explains the observed duty cycle in FRB 180916. The stripped material from the planet is then captured and accreted by the SS due to the strong magnetic field of the compact star, flowing to the polar cap region along the field lines and accumulated there. The total mass of the accreted material is estimated as $M_{acc} \simeq 4.32 \times 10^{23}$ g in each period, large enough to lead to local collapses of the crust at the polar cap region. A total energy of $E_{c,tot} \approx 2.15 \times 10^{42}$ erg will be released during the collapse. Assuming a small conversion efficiency of $\eta = 10^{-4}$, it is still sufficient to account for typical FRBs.

In our framework, the magnetosphere of the SS is filled by a small portion of the disrupted material. The resultant plasma density will gradually decrease as the accretion proceeds, leading to a decay in the characteristic oscillation frequency of the plasma. As a result, high frequency FRBs would be observed mainly in the early phase of the duty cycle, while low frequency events are observable generally at later stages. It naturally explains the frequency-dependent active window of FRB 180916. Each time a collapse occurs, a fireball consisted of a large number of electrons/positrons will be released, leading to an additional DM variation of $\sim 2\,\mathrm{pc\,cm^{-3}}$. It is also roughly consistent with the observed DM variation of FRB180916.

Note that Geng et al. [30] also tried to explain the periodically repeating FRBs by adopting the local collapse of the crust of an SS at the polar cap region. The difference in their model is that the accreted material is supplied by a companion star at a constant rate. The periodical behavior is then due to thermal-viscous instability of the accretion disk. In their framework, the period and the active window are determined by the accretion rate and the viscosity parameter. A natural result is that the period in their model may not be stable, but may vary in a relatively wide range. On the contrary, according to our modelling in this study, the FRB period is simply the orbital period of the planet, which is thus much more rigorous.

The interaction of planets/asteroids with pulsars has previously been suggested as the mechanism for producing FRBs by many authors [28,65–68]. Especially, Kurban et al. [28] studied the interaction between an NS and its planet in an elliptical orbit, where the partial disruption of the planet is also considered. The difference between those models and our current model is significant. Generally, in those models, the compact star is an NS, but not an SS. As a result, the energy mainly comes from the gravitational potential energy of the planets/asteroids (or from the Alfvén wing interaction in Kurban et al.'s [28] model). On the contrary, in our current model, the energy mainly comes from the de-confinement of normal hadronic matter at the polar cap region. Furthermore, comparing with previous studies [28–30], here we have gone further to present more details in the modeling. The frequency-dependent active window, the variation of dispersion measure and the downward drifting behavior in the frequency domain observed in FRB 180916 can all be naturally explained in our framework. Thus our modeling is a useful supplementary to the previous studies.

In our modeling, we have mentioned that it is quite possible that only a fraction of the polar cap crust will fall onto the SQM core during a collapse event. The energy released is enough to produce an FRB, especially when the radiation is highly beamed. An advantage in this case is that less material is needed to re-build the polar cap crust again. It means that more than one FRB could be produced in the duty cycle of one period. Anyway, the issue that what fraction of the polar cap crust will be destroyed during the collapse is a complicated problem and is beyond the scope of this study. It deserves further study in the future.

Recently, Li et al. [69] argued that an energetic fireball of electron/positron pairs could be erupted when a crack forms and then heals during a starquake event in neutron stars. The electrons and positrons can then produce some kinds of transients or bursts through their interaction with the magnetosphere. It is interesting to note that the collapse of the polar cap crust in our framework is somewhat like a starquake event. Similarly, an outburst might also be produced in other wavelengths, such as in X-rays and optical wavelength. However, such an outburst might be detected only when the source is not too far from us.

Acknowledgements We are grateful to the anonymous referee for valuable comments and suggestions that lead to an overall improvement of this study. We thank Chen-Ran Hu and Chen Deng for useful discussion. This study was supported by the National Natural Science Foundation of China (Grant Nos. 12233002, 12041306, 12103055, 12273113, U1938201), by the Major Science and Technology Program of Xinjiang Uygur Autonomous Region (No. 2022A03013-1), by National SKA Program of China No. 2020SKA0120300, by the National Key R&D Program of China (2021YFA0718500). YFH also acknowledges the support from the Xinjiang Tianchi Program. AK acknowledges the support from the Tianchi Talents Project of Xinjiang Uygur Autonomous Region and the special research assistance project of the Chinese Academy of Sciences.

Data availability This manuscript has no associated data or the data will not be deposited. [Authors' comment: This is a theoretical study. All the data are shown as the figures in this paper and there are no other associated animation data.]

Funded by SCOAP[3].

Appendix A: Evolution of the orbital period of a close-in binary system

In our framework, the radius of the planet will expand to adjust to a new equilibrium state after each partial disruption. The disruption radius will change correspondingly. As a result, the orbital period will also change. In our study, we follow Hamers and Dosopoulou [57] to calculate the evolution of the orbital period. The method is particularly suitable for solving the secular (i.e., orbit-averaged) changes of the orbital elements due to mass transfer in eccentric binaries.

For an interacting eccentric binary system, Hamers and Dosopoulou [57] considered two types of mass transfer: (i) The donor fills its Roche lobe during the entire orbit so that Roche lobe overflow (RLOF) takes place all the time. This is called the full RLOF case, which happens if the binary is too close-in; (ii) The donor fills its Roche lobe only during part of the orbit. It happens when the apastron is large but the orbit is very eccentric. This is called the partial RLOF case. The condition considered in our model obviously fits to their partial RLOF case.

The donor moves in an eccentric orbit defined by

$$r(\theta) = a(1 - e\cos\theta), \tag{A1}$$

where θ is the true anomaly. Partial RLOF takes place in an orbital phase range of $-\theta_c < \theta < +\theta_c$. Note that the critical phase θ_c has been defined just below Eq. (2) in the main text. Ignoring the spin of the donor star and assuming that the mass transfer is conservative, then the orbit-averaged dynamical equations can be expressed as [57]

$$\frac{\langle \dot{a} \rangle}{a} = -\frac{2\langle \dot{M}_d \rangle}{M_d} \frac{1}{f_{\dot{M}}(e,x)} \times \left[(1-q) f_a(e,x) + X_{L,0}(q) g_a(e,x) - q \frac{r_{A_a}}{a} h_a(e,x) \right], \tag{A2}$$

$$\langle \dot{e} \rangle = -\frac{2\langle \dot{M}_d \rangle}{M_d} \frac{1}{f_{\dot{M}}(e,x)} \times \left[(1-q) f_e(e,x) + X_{L,0}(q) g_e(e,x) - q \frac{r_{A_a}}{a} h_e(e,x) \right], \tag{A3}$$

where q is the mass ratio of the two objects, M_d is the mass of the donor star and $\dot{M}_d$ is its mass loss rate. r_{A_a} is the separation between the initial position of the accreted matter and the accreting star. x is the ratio of the Roche lobe radius in a circular orbit (R_L^c) to the radius of the donor,

$$x \equiv \frac{R_L^c}{R} = \frac{a}{R} \frac{0.49\, q^{2/3}}{0.6\, q^{2/3} + \ln\left(1 + q^{1/3}\right)}. \tag{A4}$$

$X_{L,0}(q)$ is the normalized position of the first Lagrange point, which can be analytically expressed as [57]

$$X_{L,0}(q) = \frac{1}{6} \times \left(-\sqrt{3} \sqrt{\frac{6\sqrt{3}(q+1)}{\sqrt{A_- + A_+ - 2q + 3}} - A_+ - \frac{q^2}{A_+} - 4q + 6} + \sqrt{3}\sqrt{A_- + A_+ - 2q + 3} + 3 \right), \tag{A5}$$

with

$$A_\pm \equiv \sqrt[3]{q\left(q^2 \pm 6\sqrt{3}\sqrt{q^2 + 27} + 54\right)}. \tag{A6}$$

The definition and detailed expressions of other functions in Equations (A2) and (A3), such as $f_{\dot{M}}(e,x)$, $f_a(e,x)$, $g_a(e,x)$, $h_a(e,x)$, $f_e(e,x)$, $g_e(e,x)$ and $h_e(e,x)$, are given below [57]:

$$\begin{aligned} f_{\dot{M}}(e,x) = -\frac{1}{96\pi} \Big[& 36e^4\theta_0 x^3 + 3e^4 x^3 \sin(4\theta_0) \\ & - 32e^3 x^3 \sin(3\theta_0) + 24e^3 x^2 \sin(3\theta_0) + 288e^2\theta_0 x^3 - 432e^2\theta_0 x^2 \\ & + 24e^2 x \left(\left(e^2+6\right)x^2 - 9x + 3\right)\sin(2\theta_0) \\ & - 24e\left(4\left(3e^2+4\right)x^3 - 9\left(e^2+4\right)x^2 + 24x - 4\right)\sin(\theta_0) \\ & + 144e^2\theta_0 x \quad + 96\theta_0 x^3 - 288\theta_0 x^2 + 288\theta_0 x - 96\theta_0 \Big], \end{aligned} \tag{A7}$$

$$\begin{aligned} f_a(e,x) = \frac{1}{96\pi} \Big[& 36e^4\theta_0 x^3 + 3e^4 x^3 \sin(4\theta_0) - 16e^3 x^3 \sin(3\theta_0) \\ & + 24e^3 x^2 \sin(3\theta_0) - 144e^2\theta_0 x^2 \\ & + 24e^2 x \left(e^2 x^2 - 3x + 3\right)\sin(2\theta_0) - 24e\left(\left(6e^2 - 8\right)x^3 \right. \\ & \left. + \left(12 - 9e^2\right)x^2 - 4\right)\sin(\theta_0) + 144e^2\theta_0 x \\ & - 96\theta_0 x^3 + 288\theta_0 x^2 - 288\theta_0 x + 96\theta_0 \Big], \end{aligned} \tag{A8}$$

$$\begin{aligned} g_a(e,x) = \frac{1}{32\pi} \Big[& 4\theta_0 x\left(e^2\left(\left(e^2-8\right)x^2 + 12\right) - 8((x-3)x+3)\right) \\ & + ex\Big\{e\Big[8\left(x\left(\left(e^2+2\right)x - 6\right) + 3\right)\sin(2\theta_0) \\ & + ex(3ex\sin(4\theta_0) \quad - 16(x-1)\sin(3\theta_0))\Big] \\ & - 16x\left(e^2(x-3) - 4x + 6\right)\sin(\theta_0)\Big\}\Big], \end{aligned} \tag{A9}$$

$$h_a(e,x) = \frac{1}{4\pi}\left[e\sin(\theta_0)\left(-\left(e^2-4\right)x^3 - \frac{4}{e\cos(\theta_0) - 1} - 12x\right)\right.$$

$$+ x\Big\{e^2(-x)(ex\sin(3\theta_0) - 3(x-2)\sin(2\theta_0)) - 2\theta_0\left(x\left(\left(e^2+2\right)x-6\right)+6\right)\Big\} + \frac{8}{\sqrt{1-e^2}}\tan^{-1}\left(\sqrt{\frac{1+e}{1-e}}\tan\left(\frac{\theta_0}{2}\right)\right)\Big], \tag{A10}$$

$$f_e(e,x) = \frac{1-e^2}{32\pi}\Big[ex\left(12e^2\theta_0x^2 + e^2x^2\sin(4\theta_0)\right) + 8ex\left(\left(e^2+3\right)x^2 - 6x + 3\right)\sin(2\theta_0)\right) - ex\left(8e(x-1)x\sin(3\theta_0) + 48\theta_0x^2 - 96\theta_0x + 48\theta_0\right) - 8(x-1)\left(\left(9e^2+4\right)x^2 - 8x + 4\right)\sin(\theta_0)\Big], \tag{A11}$$

$$g_e(e,x) = \frac{1-e^2}{48\pi e}\Big[12\theta_0\left(e^2x\left(x\left(\left(e^2+4\right)x-9\right)+6\right)-2\right) + e^2x\Big\{6\left(x\left(2\left(e^2+4\right)x-15\right)+6\right)\sin(2\theta_0) + ex(3ex\sin(4\theta_0) + (18-20x)\sin(3\theta_0))\Big\} - 6e\left(x\left(e^2x(14x-15)+8(x-3)x+24\right)-4\right)\sin(\theta_0) + 48\sqrt{1-e^2}\tan^{-1}\left(\sqrt{\frac{1+e}{1-e}}\tan\left(\frac{\theta_0}{2}\right)\right)\Big], \tag{A12}$$

$$h_e(e,x) = \frac{1}{48\pi e}\Big[\frac{e^2-1}{e\cos(\theta_0)-1}\Big\{16e^4x^3\sin(2\theta_0) + 4e^4x^3\sin(4\theta_0) - 26e^3x^3\sin(3\theta_0) + 27e^3x^2\sin(3\theta_0) + 24e^2\theta_0x^3 + 60e^2x^3\sin(2\theta_0) - 36e^2\theta_0x^2 - 126e^2x^2\sin(2\theta_0) - 12e\theta_0\left(e^2x^2(2x-3)-2\right)\cos(\theta_0) - 3e\Big[2\left(7e^2+8\right)x^3 - 3\left(3e^2+16\right)x^2 + 48x - 8\Big] \times\sin(\theta_0) + 72e^2x\sin(2\theta_0) - 24\theta_0\Big\} + 144\left(1-e^2\right)^{3/2}x\tan^{-1}\left(\sqrt{\frac{1+e}{1-e}}\tan\left(\frac{\theta_0}{2}\right)\right) + 48\sqrt{1-e^2}\left(3\left(e^2-1\right)x+1\right)\tan^{-1} \times\left(\sqrt{\frac{1+e}{1-e}}\tan\left(\frac{\theta_0}{2}\right)\right)\Big]. \tag{A13}$$

The above expressions have been implemented by Hamers and Dosopoulou into an easy-to-use PYTHON code [57], which is freely available at gethub.[3] Adopting their code and considering the conditions in our framework, we have calculated the evolution of the orbital period of the planet. The main parameters involved are taken as: $M_{\rm d} = M_{\rm planet} = 10^{-3}\,M_\odot$, $M_{\rm ss} = 1.4\,M_\odot$, $a = 0.1$ au, $e = 0.94$. Our numerical results are presented in Fig. 2 in the main text.

References

1. E. Witten, Phys. Rev. **30**, 272 (1984). https://doi.org/10.1103/PhysRevD.30.272
2. C. Alcock, E. Farhi, A. Olinto, Astrophys. J. **310**, 261 (1986). https://doi.org/10.1086/164679
3. P. Haensel, J.L. Zdunik, R. Schaefer, Astron. Astrophys. **160**, 121 (1986)
4. F. Weber, Prog. Part. Nucl. Phys. **54**, 193 (2005). https://doi.org/10.1016/j.ppnp.2004.07.001
5. J.A. Frieman, A.V. Olinto, Nature (London) **341**, 633 (1989). https://doi.org/10.1038/341633a0
6. I. Bombaci, Phys. Rev. **55**, 1587 (1997). https://doi.org/10.1103/PhysRevC.55.1587
7. K.S. Cheng, Z.G. Dai, D.M. Wei, T. Lu, Science **280**, 407 (1998). https://doi.org/10.1126/science.280.5362.407
8. Z.G. Dai, T. Lu, Phys. Rev. Lett. **81**, 4301 (1998). https://doi.org/10.1103/PhysRevLett.81.4301
9. R. Ouyed, J. Dey, M. Dey, Astron. Astrophys. **390**, L39 (2002). https://doi.org/10.1051/0004-6361:20020982
10. Y.J. Du, R.X. Xu, G.J. Qiao, J.L. Han, Mon. Not. Roy. Astron. Soc. **399**, 1587 (2009). https://doi.org/10.1111/j.1365-2966.2009.15373.x
11. Y.-F. Huang, T. Lu, Chin. Phys. Lett. **14**, 314 (1997). https://doi.org/10.1088/0256-307X/14/4/021
12. Y.F. Huang, T. Lu, Astron. Astrophys. **325**, 189 (1997)
13. J.J. Jia, Y.-F. Huang, Chin. Astron. Astrophys. **28**, 144 (2004). https://doi.org/10.1016/S0275-1062(04)90017-3
14. D.R. Lorimer, M. Bailes, M.A. McLaughlin, D.J. Narkevic, F. Crawford, Science **318**, 777 (2007). https://doi.org/10.1126/science.1147532
15. E. Petroff, J.W.T. Hessels, D.R. Lorimer, Astron. Astrophys. Rev. **27**, 4 (2019). https://doi.org/10.1007/s00159-019-0116-6
16. J.M. Cordes, S. Chatterjee, Annu. Rev. Astron. Astrophys. **57**, 417 (2019). https://doi.org/10.1146/annurev-astro-091918-104501
17. B. Marcote et al., Nature **577**, 190 (2020). https://doi.org/10.1038/s41586-019-1866-z
18. E. Petroff, J.W.T. Hessels, D.R. Lorimer, Astron. Astrophys. Rev. **30**, 2 (2022). https://doi.org/10.1007/s00159-022-00139-w
19. H. Xu et al., Nature **609**, 685 (2022). https://doi.org/10.1038/s41586-022-05071-8
20. A.E. Lanman et al., Astrophys. J. **927**, 59 (2022). https://doi.org/10.3847/1538-4357/ac4bc7
21. Y. Feng et al., Science **375**, 1266 (2022). https://doi.org/10.1126/science.abl7759
22. C. Ng, in *SF2A-2023: Proceedings of the Annual meeting of the French Society of Astronomy and Astrophysics*, pp. 37–41 (2023)
23. X.-H. Cui et al., Res. Astron. Astrophys. **21**, 211 (2021). https://doi.org/10.1088/1674-4527/21/8/211
24. W. Lu, P. Kumar, B. Zhang, Mon. Not. Roy. Astron. Soc. **498**, 1397 (2020). https://doi.org/10.1093/mnras/staa2450
25. E. Platts, A. Weltman, A. Walters, S.P. Tendulkar, J.E.B. Gordin, S. Kandhai, Phys. Rep. **821**, 1 (2019). https://doi.org/10.1016/j.physrep.2019.06.003
26. A. Vanderburg et al., Nature **526**, 546 (2015). https://doi.org/10.1038/nature15527
27. M. Jura, Astrophys. J. Lett. **584**, L91 (2003). https://doi.org/10.1086/374036
28. A. Kurban, Y.-F. Huang, J.-J. Geng, B. Li, F. Xu, X. Wang, X. Zhou, A. Esamdin, N. Wang, Astrophys. J. **928**, 94 (2022). https://doi.org/10.3847/1538-4357/ac558f
29. Y. Zhang, J.-J. Geng, Y.-F. Huang, Astrophys. J. **858**, 88 (2018). https://doi.org/10.3847/1538-4357/aabaee
30. J.-J. Geng, B. Li, Y.-F. Huang, The Innovation **2**, 100152 (2021). https://doi.org/10.1016/j.xinn.2021.100152
31. A. Kurban, X. Zhou, N. Wang, Y.-F. Huang, Y.-B. Wang, N. Nurmamat, Mon. Not. Roy. Astron. Soc. **522**, 4265 (2023). https://doi.org/10.1093/mnras/stad1260
32. J.G. Hills, Nature **254**, 295 (1975). https://doi.org/10.1038/254295a0

[3] https://github.com/hamers/emt.

33. M.J. Rees, Nature **333**, 523 (1988). https://doi.org/10.1038/333523a0
34. S. Gezari, Annu. Rev. Astron. Astrophys. **59**, 21 (2021). https://doi.org/10.1146/annurev-astro-111720-030029
35. S. van Velzen et al., Science **351**, 62 (2016). https://doi.org/10.1126/science.aad1182
36. A. King, Mon. Not. Roy. Astron. Soc. **515**, 4344 (2022). https://doi.org/10.1093/mnras/stac1641
37. M. Nikolajuk, R. Walter, Astron. Astrophys. **552**, A75 (2013). https://doi.org/10.1051/0004-6361/201220664
38. S.-F. Liu, J. Guillochon, D.N.C. Lin, E. Ramirez-Ruiz, Astrophys. J. **762**, 37 (2013). https://doi.org/10.1088/0004-637X/762/1/37
39. J.F. Sepinsky, B. Willems, V. Kalogera, Astrophys. J. **660**, 1624 (2007). https://doi.org/10.1086/513736
40. A.F. Cheng, M.A. Ruderman, Astrophys. J. **214**, 598 (1977). https://doi.org/10.1086/155285
41. E.T. Scharlemann, J. Arons, W.M. Fawley, Astrophys. J. **222**, 297 (1978). https://doi.org/10.1086/156144
42. J. Arons, E.T. Scharlemann, Astrophys. J. **231**, 854 (1979). https://doi.org/10.1086/157250
43. B. Zhang, G.J. Qiao, Astron. Astrophys. **338**, 62 (1998). arXiv:astro-ph/9806262
44. K. Kashiyama, K. Ioka, P. Mészáros, Astrophys. J. Lett. **776**, L39 (2013). https://doi.org/10.1088/2041-8205/776/2/L39
45. B. Zhang, Astrophys. J. Lett. **890**, L24 (2020). https://doi.org/10.3847/2041-8213/ab7244
46. R. Mckinven et al., Astrophys. **950**, 12 (2023). https://doi.org/10.3847/1538-4357/acc65f
47. M. Amiri et al. [CHIME/FRB], Nature (London) **582**, 351 (2020). https://doi.org/10.1038/s41586-020-2398-2
48. Q.-C. Li, Y.-P. Yang, F.Y. Wang, K. Xu, Y. Shao, Z.-N. Liu, Z.-G. Dai, Astrophys. J. Lett. **918**, L5 (2021). https://doi.org/10.3847/2041-8213/ac1922
49. N. Sridhar, B.D. Metzger, P. Beniamini, B. Margalit, M. Renzo, L. Sironi, K. Kovlakas, Astrophys. J. **917**, 13 (2021). https://doi.org/10.3847/1538-4357/ac0140
50. N.M. Batalha et al. [Kepler], Astrophys. J. Suppl. **204**, 24 (2013). https://doi.org/10.1088/0067-0049/204/2/24
51. G.W. Marcy et al., Astrophys. J. Suppl. **210**, 20 (2014). https://doi.org/10.1088/0067-0049/210/2/20
52. H.B. Perets, Z. Li, J. Lombardi, C. James, J. Milcarek, R. Stephen, Astrophys. J. **823**, 113 (2016). https://doi.org/10.3847/0004-637X/823/2/113
53. S. Bethapudi, L.G. Spitler, R.A. Main, D.Z. Li, R.S. Wharton, Mon. Not. Roy. Astron. Soc. **524**, 3303 (2023). https://doi.org/10.1093/mnras/stad2009
54. K.R. Sand et al., Astrophys. J. **956**, 23 (2023). https://doi.org/10.3847/1538-4357/acf221
55. M.S. Hjellming, R.F. Webbink, Astrophys. J. **318**, 794 (1987). https://doi.org/10.1086/165412
56. T. Bogdanović, R.M. Cheng, P. Amaro-Seoane, Astrophys. J. **788**, 99 (2014). https://doi.org/10.1088/0004-637X/788/2/99
57. A.S. Hamers, F. Dosopoulou, Astrophys. J. **872**, 119 (2019). https://doi.org/10.3847/1538-4357/ab001d
58. I. Pastor-Marazuela et al., Nature **596**, 505 (2021). https://doi.org/10.1038/s41586-021-03724-8
59. Z. Pleunis et al., Astrophys. J. Lett. **911**, L3 (2021). https://doi.org/10.3847/2041-8213/abec72
60. K. Kaur, N.C. Stone, S. Gilbaum, Mon. Not. Roy. Astron. Soc. **524**, 1269 (2023). https://doi.org/10.1093/mnras/stad1894
61. W.-Y. Wang, Y.-P. Yang, C.-H. Niu, R. Xu, B. Zhang, Astrophys. J. **927**, 105 (2022). https://doi.org/10.3847/1538-4357/ac4097
62. R. Mckinven et al., Astrophys. J. **950**, 12 (2023). https://doi.org/10.3847/1538-4357/acc65f
63. F.Y. Wang, G.Q. Zhang, Z.G. Dai, K.S. Cheng, Nat. Commun. **13**, 4382 (2022). https://doi.org/10.1038/s41467-022-31923-y
64. Z.Y. Zhao, G.Q. Zhang, F.Y. Wang, Z.G. Dai, Astrophys. J. **942**, 102 (2023). https://doi.org/10.3847/1538-4357/aca66b
65. J.J. Geng, Y.F. Huang, Astrophys. J. **809**, 24 (2015). https://doi.org/10.1088/0004-637X/809/1/24
66. Z.G. Dai, S.Q. Zhong, Astrophys. J. Lett. **895**, L1 (2020). https://doi.org/10.3847/2041-8213/ab8f2d
67. J.-J. Geng, B. Li, L.-B. Li, S.-L. Xiong, R. Kuiper, Y.-F. Huang, Astrophys. J. Lett. **898**, L55 (2020). https://doi.org/10.3847/2041-8213/aba83c
68. G. Voisin, F. Mottez, P. Zarka, Mon. Not. Roy. Astron. Soc. **508**, 2079 (2021). https://doi.org/10.1093/mnras/stab2622
69. H.-Q. Li, J.-C. Wang, Res. Astron. Astrophys. **22**, 015017 (2022). https://doi.org/10.1088/1674-4527/ac3899